

Numerical analysis of geocell reinforced ballast overlying soft clay subgrade

Sireesh Saride^{*1}, Sailesh Pradhan^{2a}, Sitharam T.G.^{2b} and Anand J. Puppala^{3c}

¹ Department of Civil Engineering, Indian Institute of Technology Hyderabad, India

² Department of Civil Engineering, Indian Institute of Science, Bangalore, India

³ Department of Civil Engineering, The University of Texas at Arlington, Texas, USA

(Received December 24, 2012, Revised February 16, 2013, Accepted March 22, 2013)

Abstract. Geotextiles and geogrids have been in use for several decades in variety of geo-structure applications including foundation of embankments, retaining walls, pavements. Geocells is one such variant in geosynthetic reinforcement of recent years, which provides a three dimensional confinement to the infill material. Although extensive research has been carried on geocell reinforced sand, clay and layered soil subgrades, limited research has been reported on the aggregates/ballast reinforced with geocells. This paper presents the behavior of a railway sleeper subjected to monotonic loading on geocell reinforced aggregates, of size ranging from 20 to 75 mm, overlying soft clay subgrades. Series of tests were conducted in a steel test tank of dimensions 700 mm × 300 mm × 700 mm. In addition to the laboratory model tests, numerical simulations were performed using a finite difference code to predict the behavior of geocell reinforced ballast. The results from numerical simulations were compared with the experimental data. The numerical and experimental results manifested the importance that the geocell reinforcement has a significant effect on the ballast behaviour. The results depicted that the stiffness of underlying soft clay subgrade has a significant influence on the behavior of the geocell-aggregate composite material in redistributing the loading system.

Keywords: ballast; geocells; model studies; numerical simulations; soft clay

1. Introduction

The presence of aggregate layer as a *supportive base layer* is a well-known component in transportation systems such as highways, rail roads and runways. The performance of the transportation systems are generally depends on the behaviour of the aggregate layer upon loading. If the subgrade soil is highly compressible, then the thickness of the aggregate layer would be very high, as per any design guideline (e.g., American Association of State Highway Transportation Officials, AASHTO or Indian Roads Congress, IRC), to avoid excessive settlements or rutting on the aggregate layer and to distribute the load uniformly. The alternative solution for this issue would be reinforcing the aggregate layer. Even though the subgrade may be firm, seasonal

*Corresponding author, Assistant Professor, E-mail: sireesh@iith.ac.in

^a Former Masters' Student, E-mail: sailesh.pp@gmail.com

^b Professor and Chair for CiSTUP, E-mail: sitharam@civil.iisc.ernet.in

^c Distinguished Teaching Professor, Associate Dean (Research), E-mail: anand@uta.edu

softening of the shallow subgrade layers from the surface, particularly after heavy rain fall events or subgrade thaw, it may be sufficient to permit a large deformation failure within the aggregate layer. Several methods may be used to increase the long term satisfactory performance of the aggregate material, one of which is the reinforcement of the aggregate layer. Decision to use any improvement technique effectively would requires a clear understanding of the behavior of granular material subjected to loading from surface or near surface.

Extensive research has been carried out using small scale/large scale model tests to improve the performance of granular base layers using geosynthetics (Giroud and Bonaparte 1984, Hass *et al.* 1988, Chan *et al.* 1989, Miura *et al.* 1990, Fereidoon and Small 1996, Indraratna and Salim 2003, Giroud and Han 2004, Reymond 2002). Several researchers have attempted to reinforce the aggregate layer using planar geogrid layers in case of rail roads (Reymond 2002, Shin and Das 2002, Indraratna and Salim 2003, Reymond and Ismail 2003, Giroud and Han 2004).

Douglas and Valsangkar (1992) carried out cycled-load testing of large-scale, model pavement structures, consisting of granular bases provided with various geosynthetics placed on peat subgrades to find out the increased stiffness of an unpaved access road structures and highlighted that the road stiffness is more appropriate parameter to be considered in the design of such roads than permanent rut depth. Raymond (2002), Raymond and Ismail (2003) have studied the effect of geogrid reinforcement on the unbound aggregates through a series of model tests under static as well as repeated loading. They considered three different methods of construction viz. uniform deposit with a single layer of geogrid, uniform deposit with two layers of geogrids and a thin strong layer of aggregate overlying a weak layer of aggregate with a planar geogrid at the interface. Out of the three construction methods, they observed that the method; uniform deposit with two geogrid layers would give better results in terms of ultimate bearing capacity. Considerable work has been carried out on fresh and recycled ballast by Indraratna and Salim (2003). They have introduced a layer of geogrid between sub-base and sub ballast to improve the performance of the rail track. They observed that the angularity of the recycled ballast would decreased by degradation due to previous loading and will resulted in higher settlement and lateral deformation compared to fresh ballast.

Recently, soil reinforcement in the form of a *geocells* has been showing its efficacy in the fields of ground modification. Geocells is a three dimensional, polymeric, honeycomb like structure of cells welded or connected at joints. The cell walls keep the encapsulated material from being pushed away from the applied load and confine the soil. Because the filled cells are connected together, the panel acts like a large mattress that spreads the applied load over an extended area leading to an improvement in the overall performance. Several investigations have been reported highlighting the beneficial use of geocell reinforcement in the construction of foundations. Rea and Mitchell (1978) and Mitchell *et al.* (1979) have carried out a series of small scale laboratory tests on loading plates supported over sand beds reinforced with square shaped paper grid cells and observed different modes of failure. Shimizu and Inui (1990) carried out load tests on hexagonal shaped single geotextile cell filled with sand overlying soft soil. Krishnaswamy *et al.* (2000) carried out a series of laboratory model tests on geocell mattress supported earth embankments constructed over a soft clay bed. Dash *et al.* (2001) investigated the reinforcing efficacy of the geocell mattress within a homogeneous sand bed supporting a strip loading plate. Dash *et al.* (2003) reported load test results on model circular loading plates supported on geocell reinforced sand beds overlying soft clay. Sitharam and Sireesh (2005) have reported load test results on model embedded circular loading plates supported on geocell reinforced beds viz. sand beds, sand overlying soft clay beds and clay beds. They observed the geocell reinforcement is more efficient

in increasing the bearing capacity of the loading plate with much reduced loading plate settlements. They have also shown that the reinforcement in the form of geocells is much superior than the planar layer of geogrid reinforcement in load carrying mechanism and controlling heave on the fill surface.

Li (2000) experimented with three different mitigating techniques to strengthen the soft subgrade section of a railroad test track under heavy axle wheel loads which include increased ballast thickness, geocell reinforced subballast and asphalt track bed stabilization. Based on the model tests, Li (2000) concluded that among the techniques considered, a granular layer with geocell improved the track performance. Raymond (2002) has reported the successful use of geocells to improve the performance of the gantry crane ballasted track through practice. Yet there is a lack of systematic study in this area.

Many a time, the difficulties involved in simulating the complexities such as stress levels anticipated in the field, material non-homogeneity and non-linear behavior of materials, influence of boundary, scale effects and limitations of 1 g model tests are resolved with numerical methods. Many researchers have simulated geogrid reinforced foundation systems using finite element methods (Yetimoglu *et al.* 1994, Peng *et al.* 2000, Boushehrian and Hataf 2003). Fagher and Jones (2001) have conducted numerical analysis to model a layer of sand blanket overlying super soft clay with a geogrid layer at its interface using FLAC and discussed the influence of the bending stiffness of the reinforcement on the bearing capacity of the super soft clay. They also studied the factors affecting the mechanisms of geogrid reinforcement.

Limited studies are available on numerical simulations of the geocell reinforced beds. Bathurst and Knight (1998) have simulated the geocell-soil reinforced conduits using GEOFEM at Royal Military College of Canada. The geocell soil layer has been modelled as an equivalent composite material having higher stiffness and shear strength. Bergado *et al.* (2000) have used finite element program to simulate the full-scale test embankment reinforced with hexagonal wire mesh. Madhavi Latha *et al.* (2001, 2009) have modelled the geocell reinforced sand beds supporting the strip loading plates by representing geocell reinforced bed as an equivalent continuum material using GEOFEM. Sitharam *et al.* (2006) and Sireesh *et al.* (2009) have shown the modelling of geocell reinforced homogeneous sand beds using a three dimensional finite difference code, FLAC 3D. In their study, the geocell was modelled using the geogrid structural elements available in the program.

In this paper, the results of a series of large scale laboratory model tests conducted on the loading plate supported on unreinforced and geocell reinforced ballast overlying compressible soft clay bed are presented. Further, these laboratory test conditions were numerically simulated using FLAC 3D, a finite difference software to capture the behaviour of the same. The results from both model tests and numerical simulations were compared.

2. Laboratory model tests

2.1 Materials used

The aggregate material used in this study is a locally available crushed aggregate consisting of mainly angular and sub-angular particles. It has a coefficient of uniformity (C_u) of 1.9, coefficient of curvature (C_c) of 0.9 and specific gravity of 2.7. The aggregate is classified as poorly graded gravel with a letter symbol GP according to the Unified Soil Classification System

Table 1 Properties of geogrid used for making geocells

Property	Value
Ultimate tensile strength	20 kN/m
Failure strain	18 %
Initial modulus	183 kN/m
Secant modulus at 5% strain	160 kN/m

(USCS). The maximum void ratio (e_{\max}) and minimum void ratio (e_{\min}) of the aggregate were found to be respectively 0.96 and 0.84. The peak friction angle obtained from large box shear tests was observed to be 55° . Soft clay subgrades were prepared using a naturally available silty clay soil, which had 60% fines fraction smaller than $75 \mu\text{m}$ sieve size. The liquid limit, plastic limit and specific gravity of the clay were found to be 40%, 17% and 2.66 respectively. As per the USCS, the clay is classified as clay with low plasticity (CL).

The geocells were formed using a biaxial geogrid made of oriented polymers. The geogrid is having a square shaped aperture opening of size $35 \text{ mm} \times 35 \text{ mm}$. The properties of the geogrid obtained from standard multi-rib tension test as per ASTM: D 6637 - 01 are listed in Table 1.

2.2 Test set-up

A test tank was designed to simulate a section of railway track and tests were conducted under static loading in a simplified and controlled manner. Fig. 1 shows the details of a typical rail track and the portion of track simulated in the present study. The model tests were conducted in a test bed-loading frame assembly in a tank with inside dimensions of $700 \text{ mm} \times 300 \text{ mm} \times 700 \text{ mm}$ (length \times width \times height). The model plate used was made of steel and measured, 300 mm length \times 250 mm width \times 8 mm thickness ($L \times B \times t$) which simulate the sleeper of a rail road. The base of the loading plate was made rough by cementing a thin layer of sand to it. The plate was centred in the tank, with the length of the plate parallel the width of the tank. In order to create plane strain

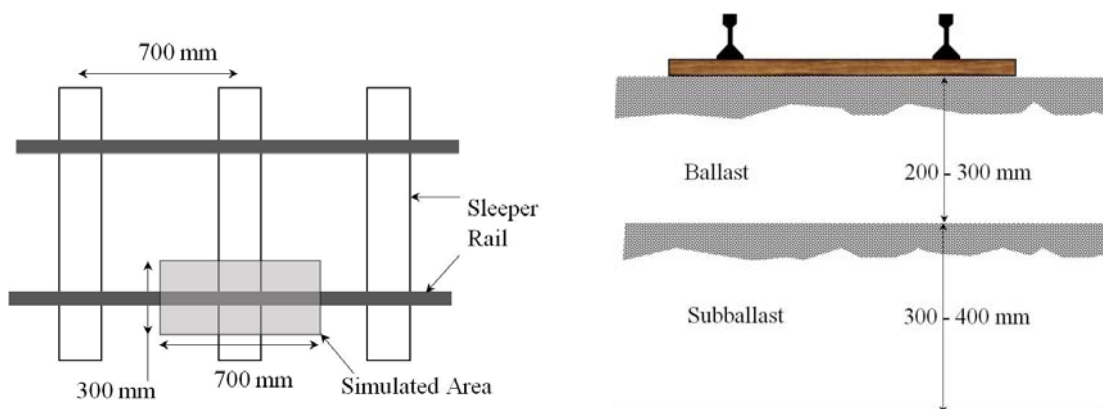


Fig. 1 Plan and sectional view of rail and sleepers showing section represented by the model test tank

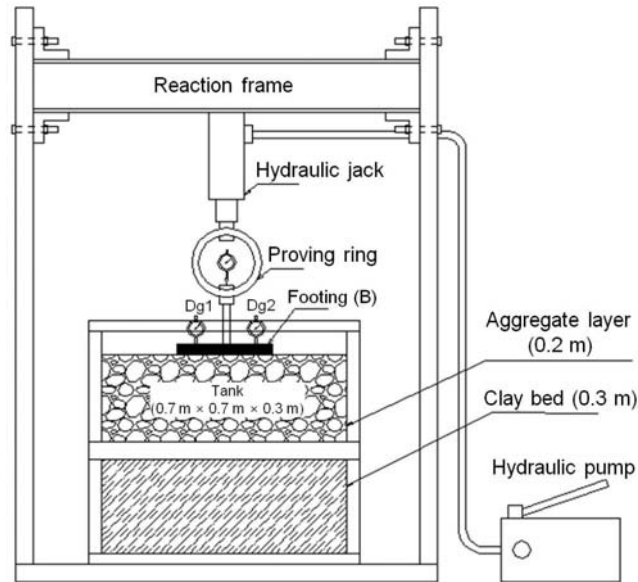


Fig. 2 Model test set-up

conditions within the test tank, length of loading plate was made nearly equal to the width of the tank. The loading plate was loaded with a hydraulic jack supported against a reaction frame as shown in Fig. 2.

2.3 Preparation of clay bed

The clay was pulverised and then mixed with predetermined amount of water. In order to achieve moisture equilibrium; the moist clay was kept in airtight containers for 7 days. To prepare the test bed, the moist clay was placed in the test tank and compacted in 25 mm thick layers till the desired height was reached. By carefully controlling the water content and compaction, a fairly uniform test condition was achieved throughout the test programme. In order to verify the uniformity of the test bed, undisturbed samples were collected from different locations and depths in the test bed to determine the in situ unit weight, moisture content and vane shear strength of the clay soil. These parameters of the compacted soil at different locations were found to be within 2 % error. Table 2 presents the average properties of the compacted moist clay at two different strength conditions during the tests.

2.4 Preparation of unreinforced and reinforced aggregate bed

Once the required depth of clay subgrades is prepared, the aggregate was placed in a 0.2 m thick layer across the tank over the prepared clay bed. Numerous trial fillings were performed to achieve a uniform placement density. In the case of geocell reinforced beds, first, the geocell mattress was prepared on top of the compacted clay bed. The geocell layer was prepared by cutting the biaxial geogrids into required length and height from full rolls and placing them in transverse

Table 2 Properties of soft clay bed

Parameter	Quantity	Quantity
Vane shear strength	6.25 kPa	16.5 kPa
Moisture content	24 %	19.7 %
Degree of saturation	100 %	100 %
Unit weight	20.47 kN/m ³	20.68 kN/m ³

and diagonal directions with bodkin joints (plastic strips) at the connections (Bush *et al.* 1990). All the geocell layers in the present investigation were prepared in square pattern. After formation of geocell layer, the geocell pockets were filled with the aggregate using hand packing technique. The densities achieved were monitored by calculating the weight of aggregate per a pre-calculated volume of each cell pocket. The placement densities for both unreinforced and geocell reinforced beds were maintained same.

2.5 Test procedure

Upon filling the tank up to the desired height, the surface was levelled and the loading plate was placed on a predetermined alignment such that the loads from the loading jack would be transferred concentrically to the loading plate. A recess was made into the loading plate at its centre to accommodate a plunger through which vertical loads were applied to the loading plate. The loading plate was pushed into the soil at a rate of nearly 2-mm per minute. The load transferred to the loading plate was measured through a pre-calibrated proving ring placed between the plunger and the loading jack. Loading plate settlements were measured through two dial gauges (Dg_1 and Dg_2) as shown in Fig. 2, placed on either side of the centre line of the loading plate. The loading plate settlement data reported here is the average values of the readings taken at two different points.

2.6 Test variables

The geocell mattresses in all the cases were formed in square shape. The pocket size (d_c) of the geocell is taken as the diameter of an equivalent circular area of the geocell pocket opening and was kept constant (0.8B) in all the tests. Height of the geocell layer (h) was varied as a height ratio, defined as a ratio of height of the geocell to the loading plate width (i.e., h/B). The height ratio was varied as 0.4, 0.6 and 0.8. The width of geocell mattress (b) was fixed based on the overall width of the tank with width of each pocket being fixed at 200 mm. A gap of 5-10 mm was maintained between the loading plate and the geocell mattress to avoid the buckling of geocell walls due to direct contact of the loading plate with geocell mattress. Three series of tests were conducted on unreinforced and geocell reinforced beds with varying compressibility of underlying soft clay subgrade and the height ratio (h/B) of the geocell mattress. The details of series of model tests are presented in Table 3. The same configuration of test beds was simulated using three dimensional finite difference program. The details of numerical simulations will be discussed in subsequent sections. Note that the tests in series C were not performed on the laboratory model scale.

Typical pressure settlement responses observed from different series of laboratory model tests on unreinforced and geocell reinforced beds are presented in Figs. 5(a), 5(b), 8(a), and 8(b)

Table 3 Details of laboratory model tests/ Numerical simulations

Test series	Type of reinforcement	Details of test parameters	
A	Unreinforced (Lab / Numerical)	Variable parameter:	$H_d/B = 0.0, 0.8$ $H_c/B = 1.2, 2.0$ $c_u = 6.25 \text{ kPa}, 16.5 \text{ kPa}$
		Constant parameter:	$\gamma_{agg} = 14.28 \text{ kN/m}^3$
B	Geocell (Lab / Numerical)	Variable parameter:	$c_u = 6.25 \text{ kPa}, 16.5 \text{ kPa}$
		Constant parameter:	$h/B = 0.8$ $\gamma_{agg} = 14.28 \text{ kN/m}^3$ $d_c/B = 0.8$ $H_c/B = 1.2$ $b/B = 2.4$
C	Geocell (Numerical)	Variable parameter:	$h/B = 0.4, 0.6, 0.8$
		Constant parameter:	$c_u = 16.5 \text{ kPa}$ $\gamma_{agg} = 14.28 \text{ kN/m}^3$ $d_c/B = 0.8$ $H_c/B = 1.2$ $b/B = 2.4$

respectively. It is inferred from Figs. 5(a) and 5(b) that in the case of unreinforced clay bed of height 500 mm, the slope of pressure settlement curve tends to become almost vertical beyond a plate settlement ratio of about 5 %. However with aggregate bed of 200 mm overlying clay bed of 300 mm, the failure could be observed at a settlement ratio of about 13 % at a bearing pressure of 135 kPa. However, the settlement profile of the bed further improved in the case of geocell reinforced aggregates overlying the clay bed. No distinct failure could be observed in this case in particular. It can be concluded that the unreinforced clay shows a clearly defined ultimate (failure) pressure, which is observed to be much lesser than the case with aggregates overlying clay subgrade.

Similar observations can also be drawn from the same Figs. for which the underlying clay has a higher shear strength, $c_u = 16.5 \text{ kPa}$ than the previous series of tests. The bearing pressure in this case of aggregate overlying clay bed is 375 kPa at a settlement ratio of 20%, where as for aggregate reinforced with geocell, again no distinct failure could be observed even at settlements of more than 25% of loading plate width and the response is almost linear. This is primarily due to very high strength rendered by the confinement of aggregates by geocell.

3. Numerical simulations

An attempt has been made to simulate the laboratory model load tests discussed in the previous sections using a three dimensional finite difference code, FLAC 3D. The numerical analysis would give a clear understanding of the mechanical behaviour of the geocell reinforced aggregate overlying soft soils. The challenge is to model the combined behaviour of coherent and complex geocell-aggregate matrix.

Table 4 Details of material properties used in numerical simulations

Material	Properties
Loading plate	$E = 2 \times 10^8$ kPa, $\mu = 0.2$
Clay, $c_u = 6.25$ kPa	$E = 0.4 \times 10^2$ kPa, $\mu = 0.3$
Clay, $c_u = 16.5$ kPa	$E = 0.55 \times 10^2$ kPa, $\mu = 0.3$
Aggregate	$E = 0.4 \times 10^3$ kPa, $\mu = 0.3$ $\phi = 55^\circ$, $c = 0$
Geogrid	Thickness of the material = 1×10^{-3} m Young's modulus, $E = 183 \times 10^3$ kPa
Interface properties:	Coupling spring stiffness per unit area, $cs_sk = 1.33 \times 10^4$ kN/m ³ Coupling spring cohesion, $cs_coh = 0$ kPa Coupling spring friction angle, $cs_fric = 30^\circ$

Both the aggregate overlying clay and the loading plate are modelled to the same scale and discretised with a primitive mesh shape 'brick' which is a graded mesh around a rectangular-shaped loading plate to maintain the compatibility between the plate and the underlying material. The behavior of the loading plate is assumed as elastic. The properties required in simulating the loading plate are presented in Table 4. The elastic-perfectly plastic Mohr-Coulomb model was used for studying the behavior of granular aggregates as well as clay. The clay behaviour is considered undrained as deformations would occur in clay bed without being drain out pore water pressure due to short term loading. The properties of clay and aggregate used in this simulation are also presented in Table 4. The geocell is modelled using the structural element, *geogrid*, which is in-built in the software. The geogrid material constitutive behavior is considered as isotropic elastic. The geocell mattress is simulated by placing the geogrid elements in transverse and lateral directions through a FISH function, a subroutine. The transverse and the lateral geogrid members are connected at predetermined coordinates to maintain the nodal

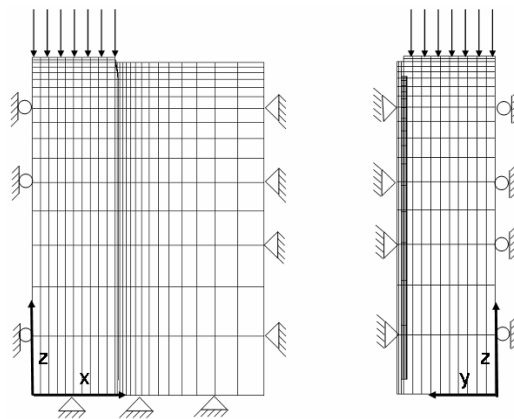


Fig. 3 Quarter symmetry model with boundary conditions considered for unreinforced bed

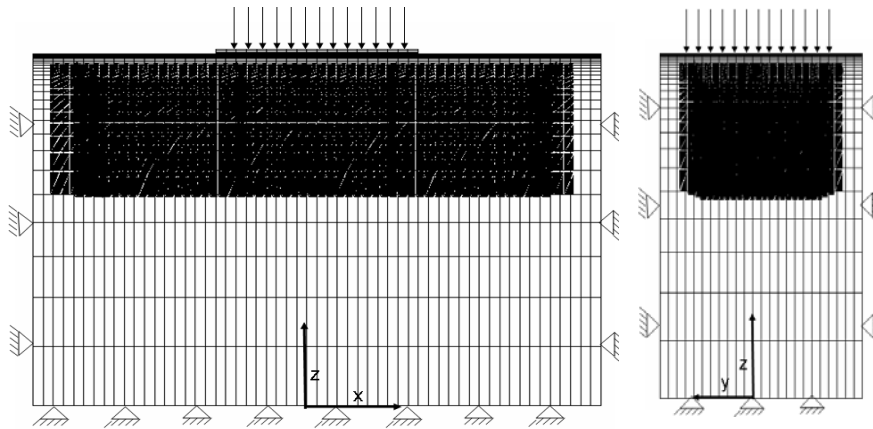


Fig. 4 Full model with boundary conditions considered for geocell reinforced bed

connectivity for representing the actual laboratory geocell mattress used in the model tests. The properties of geogrids used in the simulations are presented in Table 4.

In the case of unreinforced clay and aggregate overlying clay beds, quarter symmetric model has been considered to minimize the computational time. A domain of $0.35 \text{ m} \times 0.15 \text{ m} \times 0.5 \text{ m}$ along with boundary conditions is used in the numerical simulation to represent soil as illustrated in Fig. 3. The soil is discretised in to 5750 zones which are connected through 6830 grid points. Boundary conditions similar to that of model tests conducted in the laboratory (refer Fig. 1) have been simulated so as to compare the results. The displacements of the extreme x -, y - and z -boundaries are restricted in all directions, and the displacements of the symmetric boundaries corresponding to the planes at $x = 0$ and $y = 0$ are restricted in the x - and y - directions, respectively (as shown in Fig. 3). A downward velocity of magnitude in the range of 10^{-5} m/step was applied on top of the loading plate in the z -direction to simulate the loading. The boundary conditions applied to this domain are illustrated in Fig. 3.

In the case of geocell reinforced beds, no symmetry has been considered due to the difficulty associated with complex three-dimensional nature of geocell mattress. The model is discretised in to 40320 zones and 44175 grid points to represent the soil mass. The geocell has 12308 structural elements with 6840 nodes. The model with boundary conditions is shown in Fig. 4.

To verify the influence of boundary effects, if any, due to use of a steel test tank on laboratory model test data, numerical simulations were performed by varying the fixed extreme model boundaries at a distance of $1.4B$ and $3B$ from the centre of the loading plate. Results from this series will be discussed in subsequent sections.

4. Results and discussion

Results from numerical simulations of clay bed, ballast overlying clay bed with and without reinforcement have been compared with the model test results. The pressure-settlement responses are plotted up to about 30 % of the loading plate settlement. The displacement vectors and the stress distribution patterns obtained from the numerical analysis are also presented and discussed.

4.1 Unreinforced beds

4.1.1 Pressure settlement response

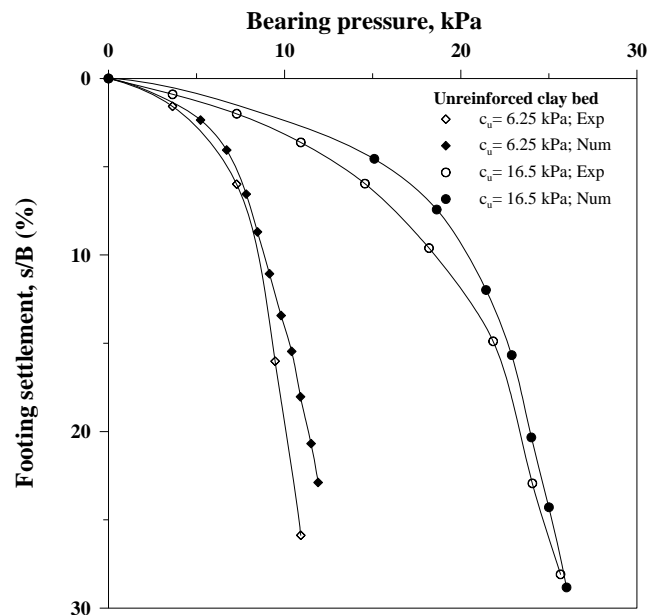
The undrained shear strength of the soft clay subgrade was varied at 6.25 kPa and 16.5 kPa in both experimental and numerical studies to understand its influence on the bearing capacity of plate resting on un-/reinforced ballast. Typical pressure settlement responses of both experimental and numerical simulations are presented in Fig. 5(a). It can be seen that the unreinforced clay bed has shown a clear failure at settlement ratios (s/B) of around 5% and 10% for c_u values of 6.25 kPa and 16.5 kPa respectively. A very close match has been observed between the experimental and the numerical results.

Similarly, Fig. 5(b) shows the variation of bearing pressure with plate settlement for both the experimental and numerical data of aggregate overlying soft clay subgrades.

A reasonably good agreement between the numerical and experimental data can be inferred from Fig. 5(b). The variation at very high settlement ratios ($s/B > 20\%$) is attributed to the uncertainty in choosing the material parameters and proper constitutive law which is inherent in any numerical analysis. It can be observed from the graph that, for aggregates overlying clay bed of c_u value 6.25 kPa and 16.5 kPa, the deviation in settlement ratios from experimental results to numerical are about 15% and 20% respectively, which are considered to be on little higher side.

4.1.2 Displacement fields and stress distribution

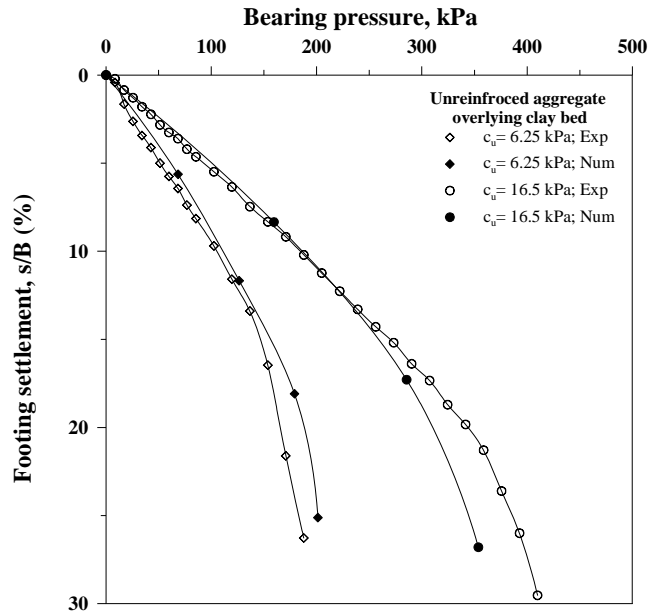
Fig. 6 presents the vertical displacement contours in z-direction (depth) for unreinforced clay bed having undrained cohesion, $c_u = 6.25$ kPa. It is clear from the Fig. 6 that the clay bed has undergone punching shear failure as the displacement colour contours show downward movement



(a) Unreinforced clay bed

Fig. 5 Continued

Fig. 5 Continued



(b) Unreinforced aggregate overlying clay bed

Fig. 5 Variation of bearing pressure with loading plate settlement for different types of clay beds (Unreinforced)

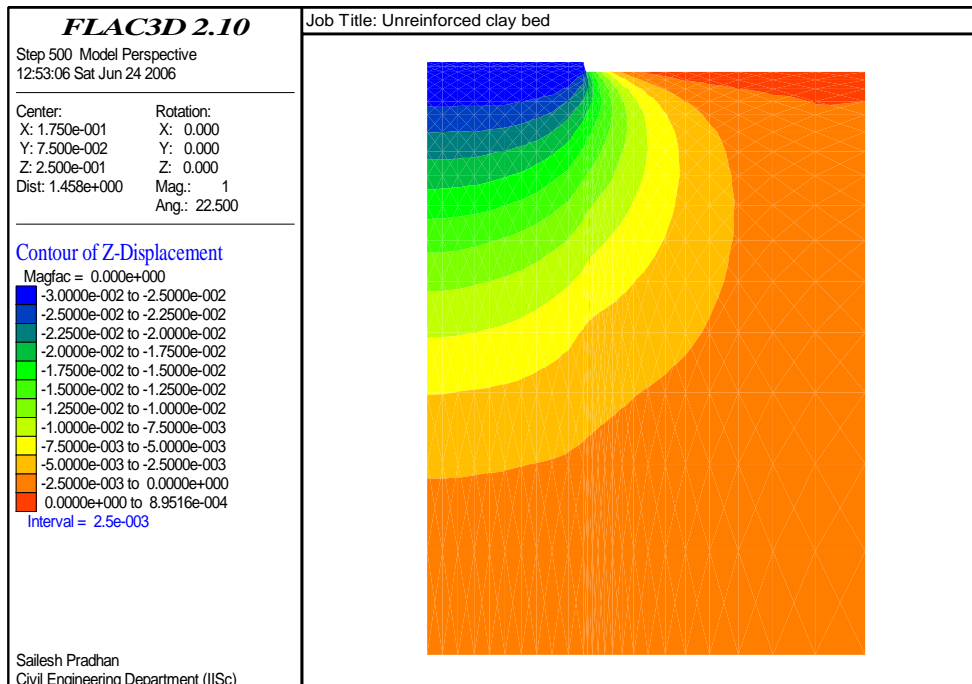
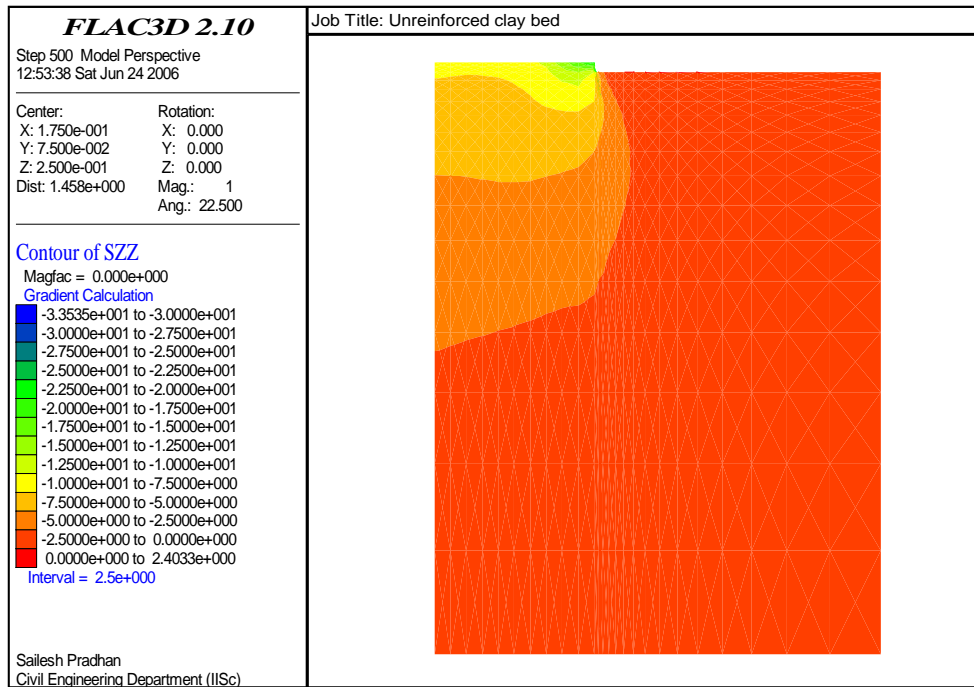
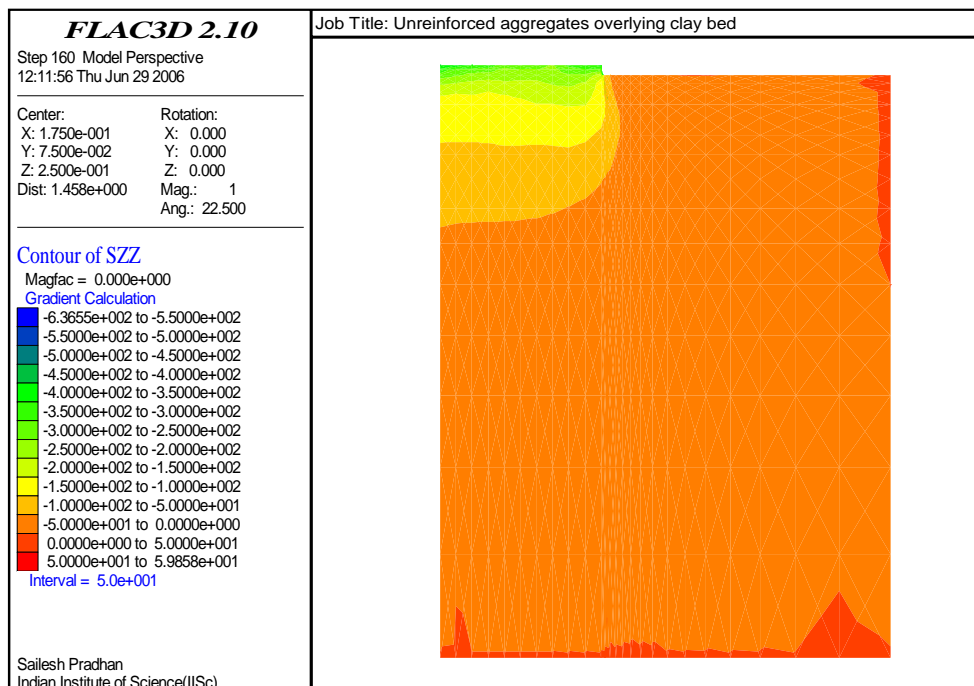


Fig. 6 Vertical displacement contours for unreinforced clay bed ($c_u = 6.25$ kPa)

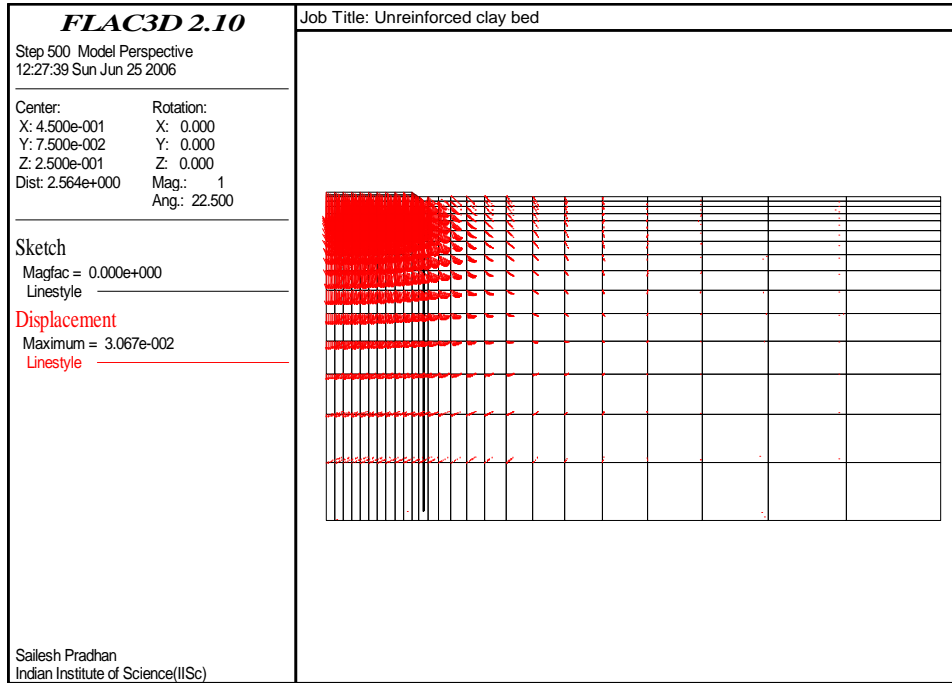


(a) Unreinforced clay bed

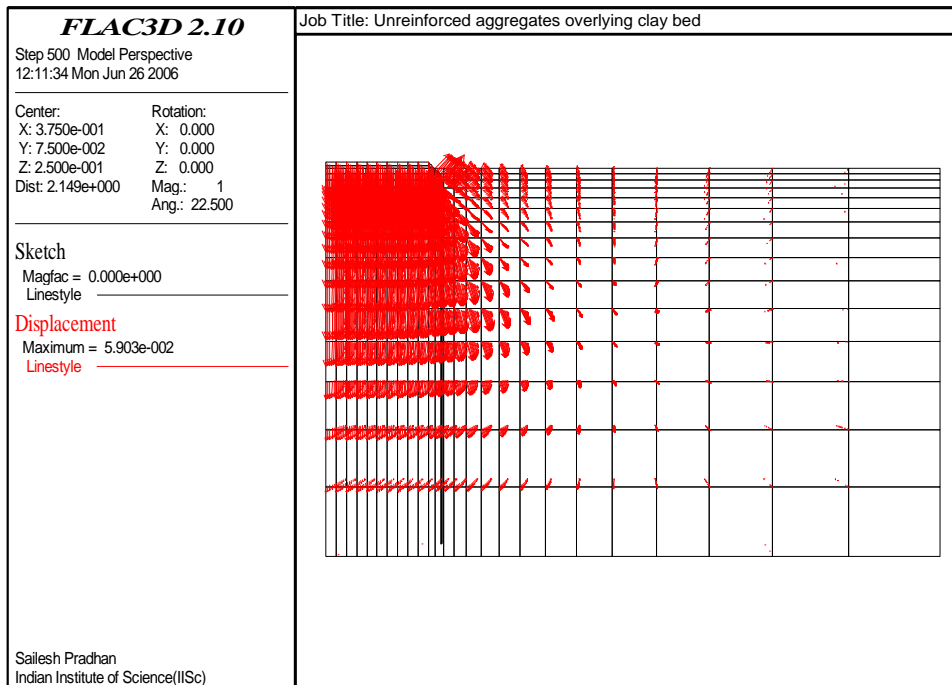


(b) Unreinforced aggregate overlying soft clay

Fig. 7 Contours of vertical displacement in (a) unreinforced clay bed; and (b) aggregate overlying clay ($c_u = 6.25$ kPa)



(a) Unreinforced homogeneous clay bed



(b) Unreinforced aggregate overlying soft clay

Fig. 8 Displacement fields in unreinforced clay and aggregate overlying soft clay for an extended boundary (3B) for $c_u = 6.25$ kPa

just below the loading plate area. The maximum displacement was observed to be 30mm under the footing. The lateral flow of the soil is very less, which is confirmed by the photographic view of the model test. Fig. 7 shows the vertical stress contours in the unreinforced clay bed and aggregate overlying soft clay bed, which indicates the contact pressure distribution at the plate-soil interface.

The lateral stresses are significant as expected because of lack of lateral restraint. The qualitative observation from this Fig. is to read the depth of soil under influence. In the case of unreinforced clay bed, the soil under the depth of influence is higher than in the case of aggregate overlying soft clay. This is only a qualitative observation as the contact pressure in two cases is different.

4.1.3 Effect of fixed boundary

It is apparent that in laboratory model tests, the fixed boundaries of steel test tank may influence the behaviour of the reinforced bed. To understand the effect of fixed boundary on the performance of the system, the extreme fixed boundaries in the numerical simulations are taken to a large distance (three times the footing width, 3B) from the centre line of the loading plate. Fig. 8 depicts the influence of extended right side boundary from 1.4B to 3B on the displacement behaviour of the unreinforced homogeneous clay and unreinforced aggregate overlying soft clay subgrades. It can be observed from the Fig. 8, that the displacement fields in both the beds are same as it appeared in the case of boundaries at 1.4B. It can also be deduced that the displacements are quite concentrated in the top aggregate layer than in the underlying soft clay. It indicates that most of the pressure from the loading plate is transmitted to the aggregate layer due to the thickness of aggregate layer. This indicates that the influence of fixed right boundary on the behaviour of homogeneous clay as well as aggregate overlying soft subgrades is negligible and

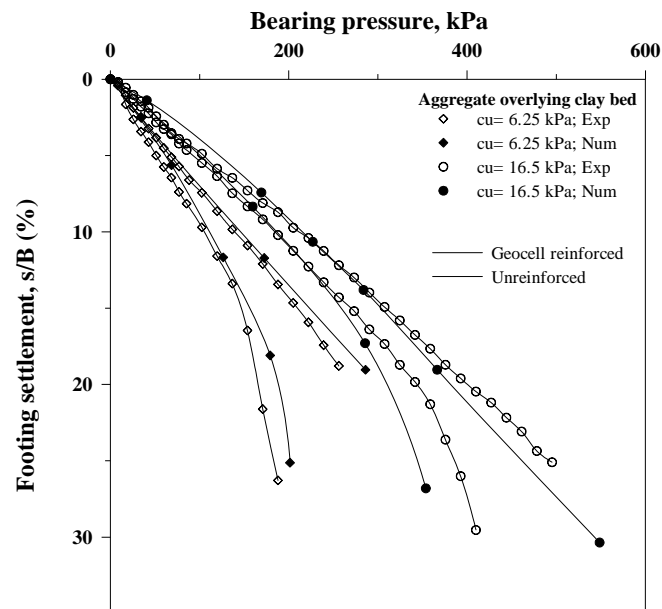


Fig. 9 Pressure-settlement responses for geocell reinforced and unreinforced aggregate overlying soft clay beds

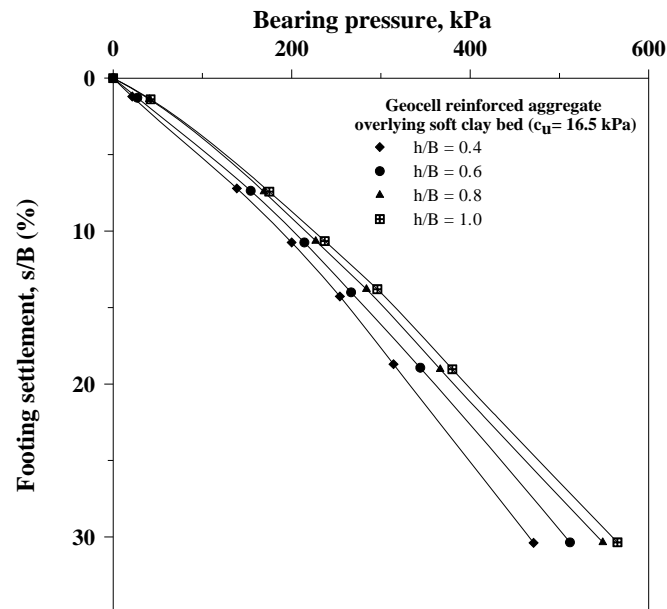


Fig. 10 Variation of bearing pressure with footing settlement for different heights of geocell mattress

hence the test results are independent of the boundary effects observed from numerical simulations as well as laboratory tests.

4.2 Geocell reinforced aggregates overlying clay bed

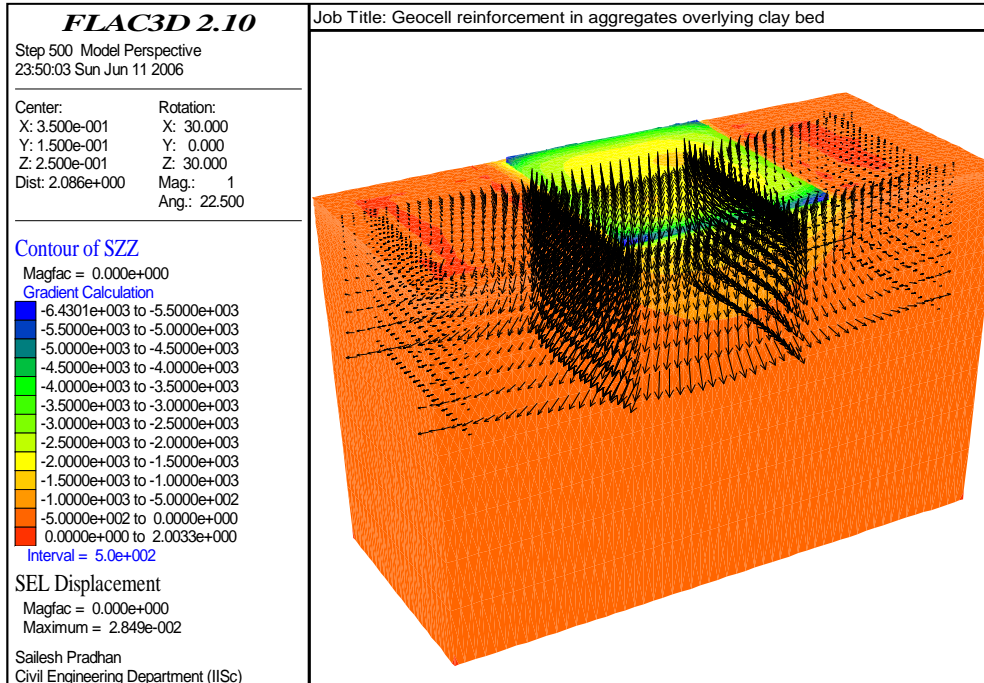
4.2.1 Pressure settlement response

Fig. 9 shows the behavior of geocell reinforced aggregate overlying clay beds for $c_u = 6.25$ kPa and 16.5 kPa. For unreinforced beds, the stiffness of the bed has decreased at about 15% of the plate width. A clear failure is not noticed even up to a plate settlement as high as 30% for reinforced cases. Besides, the pressure-settlement responses with geocell reinforcement are found to be much stiffer compared to the unreinforced cases indicating that the geocell reinforcement can reduce the settlements substantially. It can also be depicted that for relatively weaker subgrade with $c_u = 6.25$ kPa, the numerical results are slightly over estimating the pressure which was found otherwise for relatively stronger subgrade with $c_u = 16.5$ kPa.

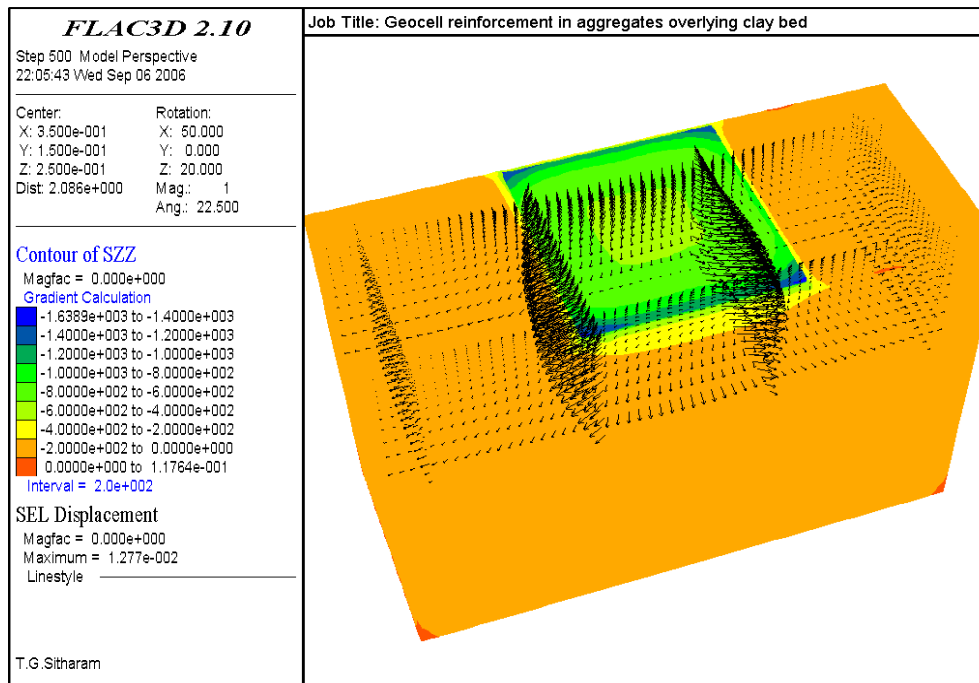
Numerical simulations were performed for increased height of geocell mattresses to understand its efficacy in improving the performance. Experimental results were not available for this series of experiments. The stiffness of the system is increased with an increase in the height of the geocell mattress from $h/B = 0.4$ to 0.8 as shown in Fig. 10. Further increase in height of the geocell has not shown much performance improvement indicating that the effective height of the geocell for this case would be 0.8B. The limited performance improvement of the system with increased height of geocell can be attributed to the relatively stronger clay subgrade with $c_u = 16.5$ kPa.

4.2.2 Displacement fields and stress distribution

The displacements in the geocell mattress combined with the vertical stress distribution in the



(a) Geocell reinforced aggregate overlying soft clay ($c_u = 6.25$ kPa)



(b) Geocell reinforced aggregate overlying soft clay ($c_u = 16.5$ kPa)

Fig. 11 Geocell displacement and vertical stress distribution (S_{zz}) in the aggregate bed overlying clay for (a) 6.25 kPa; and (b) 16.5 kPa

geocell reinforced ballast bed are presented in Figs. 11(a) and 11(b). Fig. 11(a) pertains to the clay bed prepared at $c_u = 6.25$ kPa and Fig. 11(b) for $c_u = 16.5$ kPa. It can be clearly deduced from these Figures that the displacements are higher in the central geocell pockets than the adjacent cell pockets. These displacements are high in geocell mattress over softer subgrade ($c_u = 6.25$ kPa) than the relatively stiffer clay subgrade ($c_u = 16.5$ kPa). The extreme cell displacements are as high as 28.5 mm in the case of softer subgrades against 12.7 mm in stiffer subgrade. The reduction in displacements is more than 50 % in the case of relatively stiffer subgrades.

It is also interesting to note that the lateral displacement (bulging) of central geocell pocket immediately below the loading area was very high when compared to the adjacent cell pockets. In general, the geocell pockets supposed to withstand the lateral deformation of the infill material thus providing the structural support through the hoop stresses to the loading system. However, in the present case, the number of geocell pockets adjacent to the central cell is limited to one on either side. This might have brought down the lateral support to the central geocell pocket. The undrained cohesion of the soft clay subgrade has also an impact on the performance of the geocell reinforced ballast. These lateral displacements in the central cell pocket are higher in the weaker subgrades. The geocell reinforcement system, being an interconnected like a cage, derives tremendous anchorage from both sides of the loaded area due to frictional and passive resistance developed at the soil geocell interfaces. Further, because of the shear and flexural rigidity, the geocell layer supports the loading plate even after failure of the materials inside the pockets below the loading area. The stress concentration under the plat reveals that a higher contact pressure of 6.4 kPa is noted at the edge of the footing against a pressure of 2 kPa noted at the centre of the loading plate in the case of geocell reinforced aggregate with relatively softer subgrade. This trend is common for weaker cohesive soils under rigid loading which confirms that the supporting soil in the present case is weaker. In the case of relatively stiffer subgrade, the trend of pressure distribution confirms to the loose-dense soil under a rigid loading. It can be summarised from the vertical stress distribution patterns that the performance of the geocell reinforcement is influenced by the stiffness of the soft subgrade layer.

5. Conclusions

Based on the results obtained from numerical analysis as well as laboratory model tests, the following conclusions are drawn.

A close match has been observed between the numerical and model test results in the case of unreinforced beds. Based on the numerical results, it could be inferred that the rigid boundaries simulated in the experimental studies have no significant influence on the series of experimental results. For geocell reinforced aggregate bed, it could be observed that the height of geocell has a considerable effect on the bearing capacity of the loading plate. Higher bearing capacities were noticed for higher thickness of geocell mattress. Similarly, it could be observed from the displacement plots that the surface deformations are clearly noticed for unreinforced aggregates overlying clay bed whereas deformations are contained in the case of geocell reinforcement.

The performance of the geocell reinforcement is completely depends on the stiffness of the underlying soft clay subgrade. For relatively weaker subgrades, there is an excessive vertical and lateral deformation than in the case of relatively stiffer subgrades. These deformations are attributed to the reduced modulus of subgrade reaction for weaker subgrades. The optimum height of the geocell reinforced aggregate for this case was observed to be 0.8B. Further increase in

height of the geocell did not show much improvement in terms of the stiffness of the system.

However, the extrapolation of the results from these model tests and numerical analysis to the field cases should be done carefully as the performance of the loading plates on granular materials is also dependent on the size of the loading plate (Das *et al.* 1996).

Overall, it could be inferred that the ballast can be reinforced with the three dimensional geocell mattresses to avoid lateral spreading and to improve the load carrying capacity. The finite difference code is capable of modelling the complex aggregate-reinforcement system successfully.

References

- Bathurst, R.J. and Knight, M.A. (1998), "Analysis of geocell reinforced-soil covers over large span conduits", *Comput. Geotech.*, **22**(3/4), 205-219.
- Bergado, D.T., Teerawattanasu, C., Youwai, W. and Vottipruex, P. (2000), "Finite element modeling of hexagonal wire reinforced embankment on soft clay", *Can. Geotech. J.*, **37**(6), 1209-1226.
- Boushehrian, J.H. and Hataf, N. (2003), "Experimental and numerical investigation of the bearing capacity of model circular and ring footings on reinforced sands", *Geotext. Geomembranes*, **21**(4), 241-256.
- Bush, D.I., Jenner, C.G. and Bassett, R.H. (1990), "The design and construction of geocell foundation mattress supporting embankments over soft ground", *Geotext. Geomembr.*, **9**(1), 83-98.
- Chan, F., Barksdale, R.D. and Brown, S.F. (1989), "Aggregate base reinforcement of surfaced pavements", *Geotext. Geomembr.*, **8**(3), 165-189.
- Dash, S.K., Krishnaswamy, N.R. and Rajagopal, K. (2001), "Bearing capacity of strip footings supported on geocell-reinforced sand", *Geotext. Geomembr.*, **19**(4), 235-256.
- Dash, S.K., Sireesh, S. and Sitharam, T.G. (2003), "Model studies on circular footing supported on geocell reinforced sand underlain by soft clay", *Geotext. Geomembr.*, **21**(4), 197-219.
- Douglas, R.A. and Valsangkar, A.J. (1992) "Unpaved stiffness geosynthetic-built resource access roads: Rather than Rut depth as the key design criterion", *Geotext. Geomembr.*, **11**(1), 45-59.
- Fakher, A. and Jones, C.J.F.P. (2000), "When the bending stiffness of geosynthetic reinforcement is important", *Geosynth. Int.*, **8**(5), 445-460.
- Fereidoon, M.N. and Small, J.C. (1996), "Effect of geogrid reinforcement on model track tests on pavements", *J. Transport. Eng., ASCE*, **12**(6), 468-474.
- Giroud, J.P. and Bonaparte, R. (1984), "Design of unpaved roads and trafficked areas with geogrids," *Proceeding of Symposium on Polymer Grid Reinforcement*, Science and Engineering research Council and Netlon Ltd., London, 166-127.
- Giroud, J.P. and Han, J. (2004a), "Design method for geogrid-reinforced unpaved roads. I. Development of design method", *J. Geotech. Geoenviron. Eng., ASCE*, **130**(8), 775-786.
- Giroud, J.P., and Han, J. (2004b), "Design method for geogrid-reinforced unpaved roads. II. Calibration and applications", *J. Geotech. Geoenviron. Eng., ASCE*, **130**(8), 787-797.
- Hass, R., Walls, J. and Carroll, R.G. (1988), "Grid reinforcement of granular bases in flexible pavements", *Transport. Res. Rec.*, **1188**, Transportation Research Board, Washington, D.C., 19-27.
- Indraratna, B. and Salim, W. (2003), "Deformation and degradation mechanics of recycled ballast stabilised with geosynthetics", *Soil. Found.*, **43**(4), 35-46.
- Krishnaswamy, N.R., Rajagopal, K. and Madhavi Latha, G. (2000), "Model studies on geocell supported embankments constructed over soft clay foundation", *Geotech. Test. J., ASTM*, **23**(1), 45-54.
- Latha, G., Dash, S.K. and Rajagopal, K. (2009), "Numerical simulation of the behavior of geocell reinforced sand in foundations", *Int. J. Geomech., ASCE*, **9**(4), 143-152.
- Latha, G., Dash, S.K., Rajagopal, K. and Krishnaswamy, N.R. (2001), "Finite element analysis of strip footing on geocell reinforced sand beds", *Ind. Geotech. J.*, **31**(4), 454-478.
- Li, D. (2000), "Deformations and remedies for soft railroad subgrade subjected to heavy axle loads", *Adv. Transport. Geoenviron. Syst. Using Geosynth., ASCE*, Reston, 307-321.

- Mitchell, J.K., Kao, T.C. and Kavazanjian, Jr. E. (1979), *Analysis of grid cell reinforced pavement bases*, Technical Report No. GL-79-8, U.S. Army Waterways Experiment Station, Vicksburg, MS.
- Miura, N., Sakai, A. and Taesiri, Y. (1990), "Polymer grid reinforced pavement on soft clay grounds", *Geotext. Geomembr.*, **9**(1), 99-123.
- Peng, F., Kotake, N., Tatsuoka, F., Hirakawa, D. and Tanaka, T. (2000), "Plane strain compression behaviour of geogrid-reinforced sand and its numerical analysis", *Soil. Found.*, **40**(3), 55-74.
- Raghavendra, H.B. (1996), "Some studies on the analysis of reinforced soil beds", Ph.D. Thesis, Department of Civil Engineering, *Ind. Inst. Sci.*, Bangalore, India.
- Raymond, G.P. (2002), "Reinforced ballast behavior subjected to repeated load", *Geotext. Geomembr.*, **20**(1), 39-61.
- Raymond, G.P. and Ismail, I. (2003), "The effect of geogrid reinforcement on unbound aggregates", *Geotext. Geomembr.*, **21**(6), 355-380
- Rea, C. and Mitchell, J.K. (1978), "Sand reinforcement using paper grid cells", *ASCE Spring Convention and Exhibit*, Preprint 3130, Pittsburgh, PA, April, 24-28.
- Shimizu, M. and Inui, T. (1990), "Increase in the bearing capacity of ground with geotextile wall frame", *Proceedings of the 4th International Conference on Geotextiles Geomembranes and Related Products*, Hague, Netherlands, May.
- Shin, E.C., Kim, H.D. and Das, B.M. (2002), "Geogrid reinforced rail road bed settlement due to cyclic load", *Geotech. Geol. Eng.*, **20**(3), 261-272.
- Sireesh, S., Srilakshmi, G., Sitharam, T.G. and Puppala, A.J. (2009), "3D numerical simulation of geocell reinforced soil beds", *Ground Improv. J., Proceedings of ICE*, **162**(4), 185-198.
- Sitharam T.G. and Sireesh S. (2005), "Behavior of embedded footings supported on geocell reinforced foundation beds", *Geotech Test. J., ASTM*, **28**(5), 452-463.
- Sitharam, T.G., Srilakshmi, G. and Saride, S. (2006), "Numerical simulation of geocell reinforced sand Beds using FLAC3D", *Proceeding of 4th International FLAC Symposium on Numerical Modeling in Geomechanics – Hart & Varona* (eds.) Paper: 05-04, © 2006 Itasca Consulting Group, Inc., Minneapolis, ISBN 0-9767577-0-2.
- Yetimoglu, T., Wu, J.T.H. and Saglamer, A. (1994), "Bearing capacity of rectangular footing on geogrid reinforced sand", *J. Geotech. Eng., ASCE*, **120**(12), 2083-2099.